ELSEVIER

Journal of Food Engineering **33** (1997) 151–165

PII: S0260-8774(97)00046-0 0260-8774/97 $17.00+0.00

Visualization of the Flow Patterns in a High-pressure Homogenizing Valve Using a CFD Package

Matthew J. Stevenson & Xiao Dong Chen*

Food Science and Process Engineering Group, Department of Chemical & Materials Engineering, The University of Auckland, Private Bag 92019, Auckland, New Zealand

(Received 15 November 1996; accepted 10 May 1997)

ABSTRACT

Visualization of the flow in a homogenizing valve was investigated using a commercial Computational Fluid Dynamics (CFD) code. The modeling showed that the valve can be modeled by CFD and that the resulting information compared well to results of previous experimental and theoretical investigations. The modeling gives the first detailed information available on the high fluid speeds in disruption valves. A possible use of the information obtained is to produce models for cell and fat globule disruption based on basic flow variables. The modeling gives the benefit of 'quick' estimation of flow, rather than having to use physical tests. © 1997 Elsevier Science Limited.

NOTATION

ε	Turbulence energy dissipation (m^2/s^3)
ε_{in}	ε into valve inlet (boundary condition)
k	Turbulence kinetic energy (m^2/s^2)
k_{in}	k into valve inlet (boundary condition)
μ	Laminar viscosity (Pa s)
μ_{eff}	Effective viscosity (Pa s)
μ_T	Turbulent viscosity (Pa s)
ν	Kinematic viscosity (m^2/s)
ϕ	General variable solved, e.g. u, v, k
ϕ_{new}	Variable used in next iteration
ϕ^*_{new}	Variable from solving equations
ϕ_{old}	Variable from previous iteration
ψ	Under relaxation parameter

*To whom all correspondence should be addressed.

ρ	Density (kg/m^3)
σ_k	Turbulent Prandtl number for k
σ_ε	Turbulent Prandtl number for ε
ζ	Bulk viscosity (Pa s)
C	Coefficient in exit loss equation
C_μ	Turbulent model constant (0.09)
C_1	Turbulent model constant (1.44)
C_2	Turbulent model constant (1.92)
D	Pipe diameter (m)
h	Valve gap (m)
k_e	Exit loss coefficient
k_f	Friction loss coefficient
k_i	Entrance loss coefficient
p	Pressure (Pa)
p'	Modified pressure
P	Shear production
Q	Volumetric flow (m^3/s)
r_i	Radius at valve gap inlet (m)
r_e	Radius at valve gap exit (m)
Re	Reynolds number
t	time (s)
U	Velocity vector
$\bar{u}_i$	Velocity at valve gap inlet (m/s)
u, v	Cartesian velocity components
$\nabla\cdot$	Divergence operator
∇	Gradient operator
$\otimes$	Tensor product $(A \otimes B)_{ij} = A_i B_j$
$(\cdot)^T$	Transpose of matrix, e.g. $(U)^T$ where ∇U implies

$$\begin{pmatrix} u_x & u_y & u_z \\ v_x & v_y & v_z \\ w_x & w_y & w_z \end{pmatrix}$$

INTRODUCTION

High-pressure homogenizing and cell-disruption valves play an important role in a variety of industries. Uses range from the homogenizing of milk fat globules in the dairy industry to breakage of cell walls in many biological processes. This investigation aims to model a valve using a commercially available Computational Fluid Dynamics (CFD) package such that the detailed flow patterns in the valve can be visualized.

The simulation was firstly validated against previous experimental studies (Kleinig *et al.*, 1995). Further study was then undertaken to obtain a better understanding of the flow patterns in the valve which can not easily be resolved experimentally. The detailed information can be used to understand the mechanisms of globule breakup or cell disruption in valves in future work.

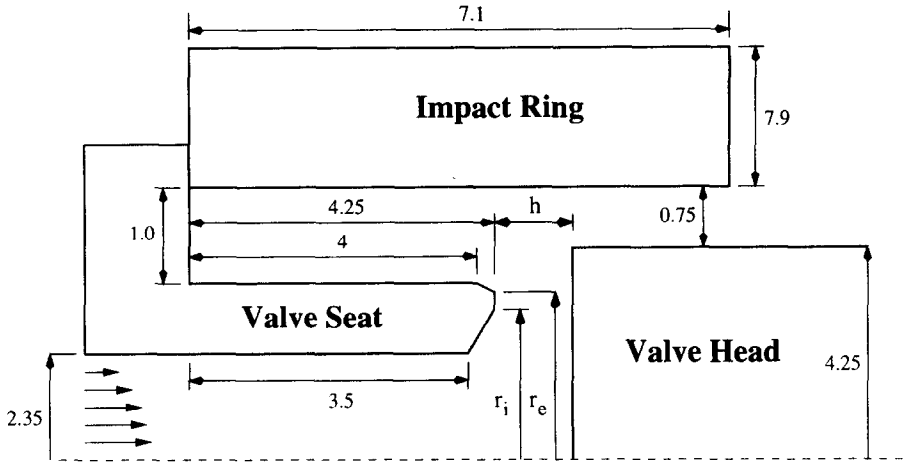

Fig. 1. Valve geometry (dimensions in cm).

The valve modeled was that used in an experimental investigation by Kleinig *et al.* (1995), the APV-Gaulin Cell-Disruption valve as shown in Fig. 1. The valve gap is greatly expanded on the diagram to allow for better visualization. The study by Kleinig *et al.* (1995) looked at very small valve gaps of 8 to 25 μm, for which experiments were carried out to determine the pressure drops across the valve. The results from this study were firstly compared to other theoretical and experimental results of Nakayama (1964), Kawaguchi (1971) and Phipps (1974a, b, 1975). This provides confidence with the CFD simulation.

A general summary of the existing methods for determining the pressure drop across valves has been given by Kleinig *et al.* (1995). The pressure loss across the whole valve consists of three parts, an entrance loss, an exit loss and a frictional loss:

$$\frac{2\Delta p}{\rho \bar{u}_i^2} = k_i + k_f + k_e \tag{1}$$

The entrance loss coefficient k_i is given the values by Phipps (1975) of 0.5 for a sharp entrance and 0.2 for a round entrance. A value of 0.2 was used in the following analysis to be consistent with Kleinig *et al.* (1995).

Nakayama (1964) derived an equation for k_f based on laminar flow, which is given by eqn (2).

$$k_f = \frac{12}{mRe} \ln\left(\frac{r_e}{r_i}\right) \tag{2}$$

where

$$m = \frac{h}{2r_i}$$

$$Re = \frac{\bar{u}_i h}{\nu} = \frac{Q}{2\pi r_i \nu}$$

Kawaguchi (1971) used a 1/7 turbulent velocity profile and derived equation for k_f as given by

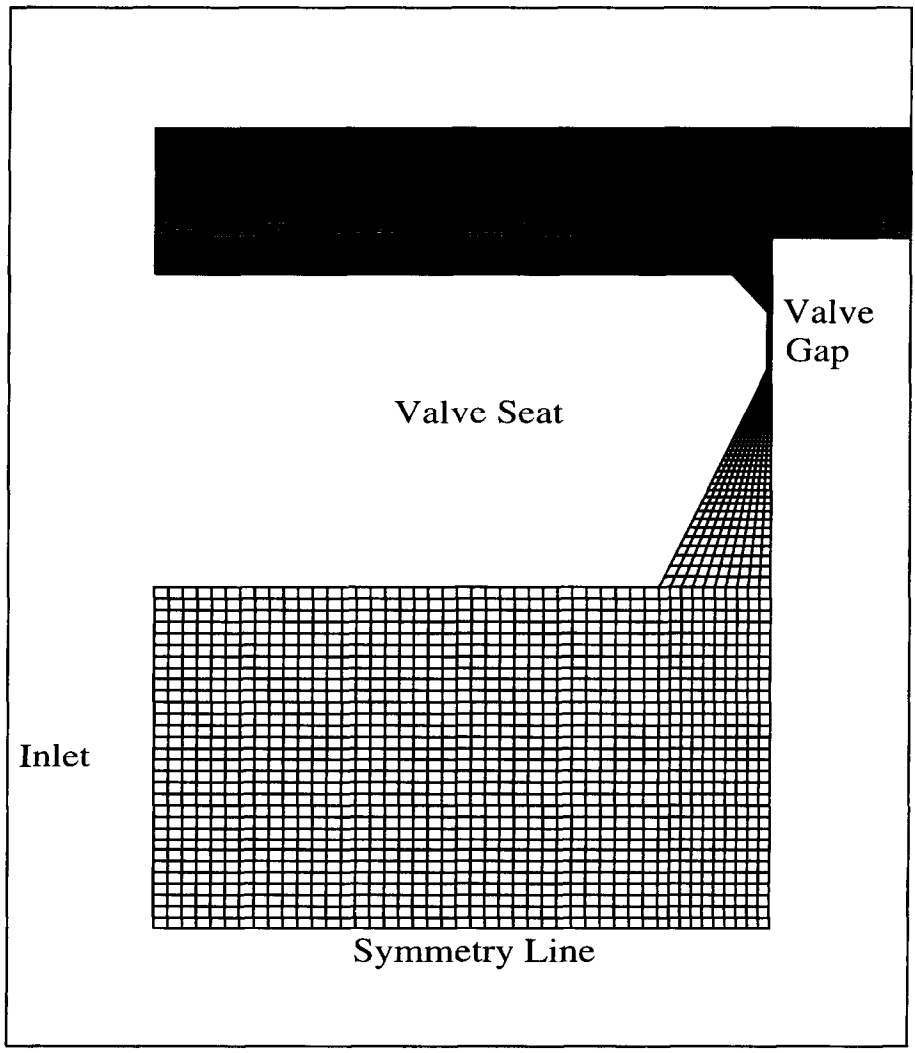

Fig. 2. Grid for 30 μm valve gap.

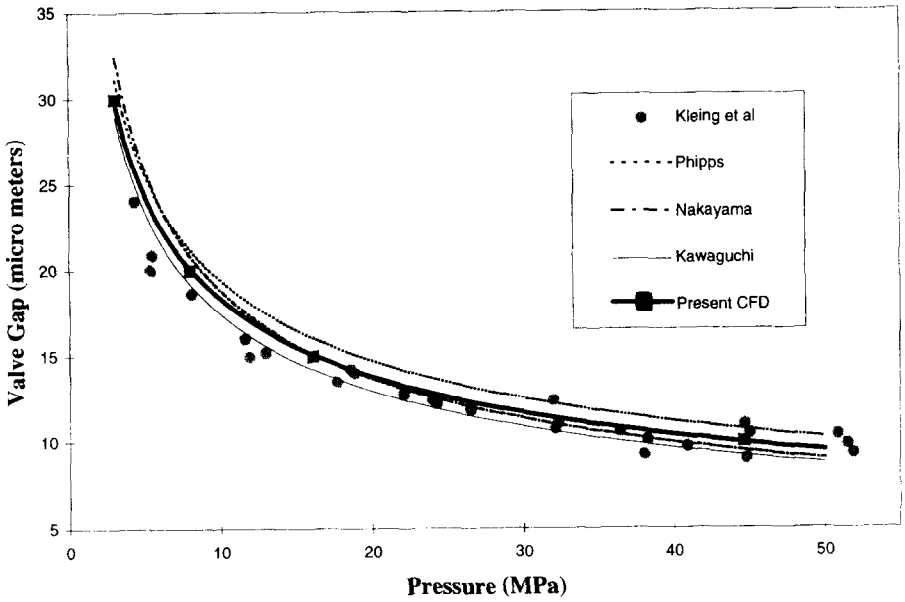

Fig. 3. Pressure drop across valve theoretical and experimental results.

$$k_f = \frac{0.076}{m(Re/2)^{1/4}}\left(1-\left(\frac{r_i}{r_e}\right)^{3/4}\right) \tag{3}$$

Phipps (1975) developed an empirical relationship for Reynolds numbers in the range 1,000–5,000. The relationship was given by eqn (4):

$$k_f = \frac{0.076}{m(Re/2)^{3/5}}\left(1-\left(\frac{r_i}{r_e}\right)^{2/5}\right) \tag{4}$$

The exit loss coefficients can be determined from eqn (5).

$$k_e = C\left(\frac{r_i}{r_e}\right) \tag{5}$$

The coefficient C was assumed to have the value of 1.0 by Phipps (1975). Nakayama (1964) derived the value of 54/35. Kawaguchi (1971) used a value of 64/63. As can be seen, all these analytical models require empirical constants to be determined, by comparing the predictions with lab test results. For different valve geometry, these constants need to be re-validated experimentally. It is shown in this work that this

may be avoided using a full scale computational analysis involving the detailed fluid mechanics in the valve.

THE COMPUTATIONAL FLUID DYNAMICS MODEL

A homogenizing or cell disruption valve is operated typically under transient mode. This is because the high operating pressure > 40 MPa requires a single or multi-stage piston pump. The pump causes both a change in the flow rate and the valve gap during each pump cycle. However, from the experiments of Kleinig *et al.* (1995) it was seen that a significant portion of each cycle is at a reasonably steady pressure and valve gap. During that portion of time the valve operation can be modeled as

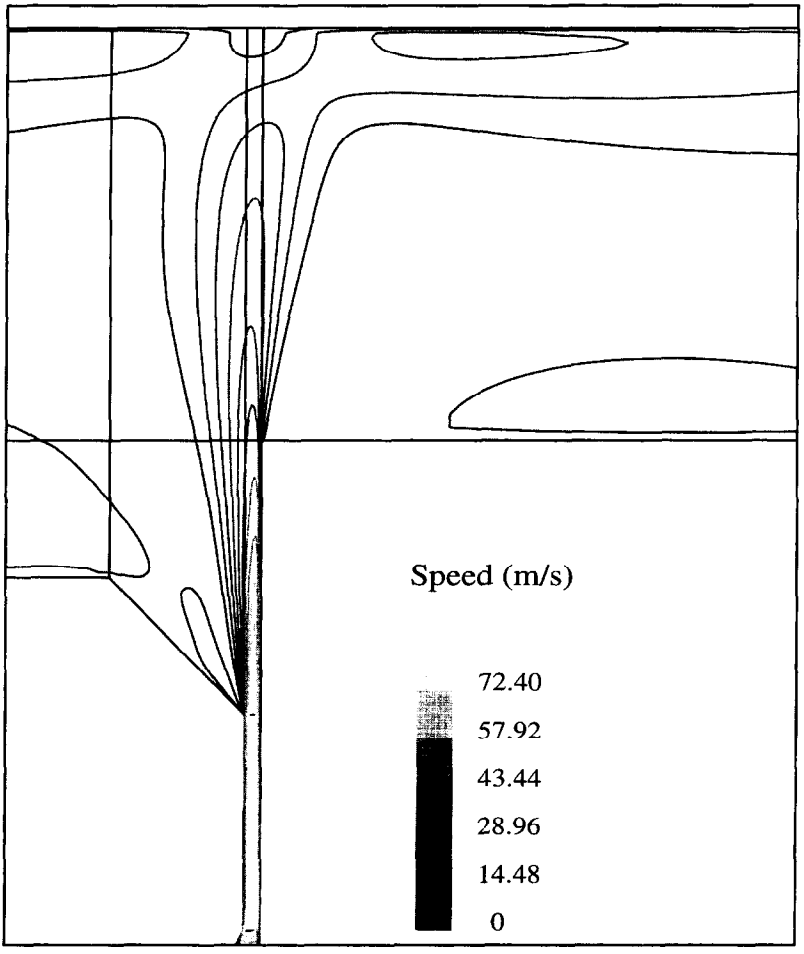

Fig. 4. Velocity contours, 30 μm valve gap.

a steady state device. Modeling as steady state allowed much shorter computation times.

The computational fluid dynamics investigation of the valve was performed using Flow 3D 3.1.2, which is a general purpose finite volume code that can be used for both incompressible and compressible fluids. The standard form of the $k-\varepsilon$ turbulence model of Launder & Spalding (1974) was used in this work. The fundamental equations are:

$$Continuity \quad \frac{\partial \rho}{\partial t} + \nabla \cdot (\rho U) = 0 \tag{6}$$

and

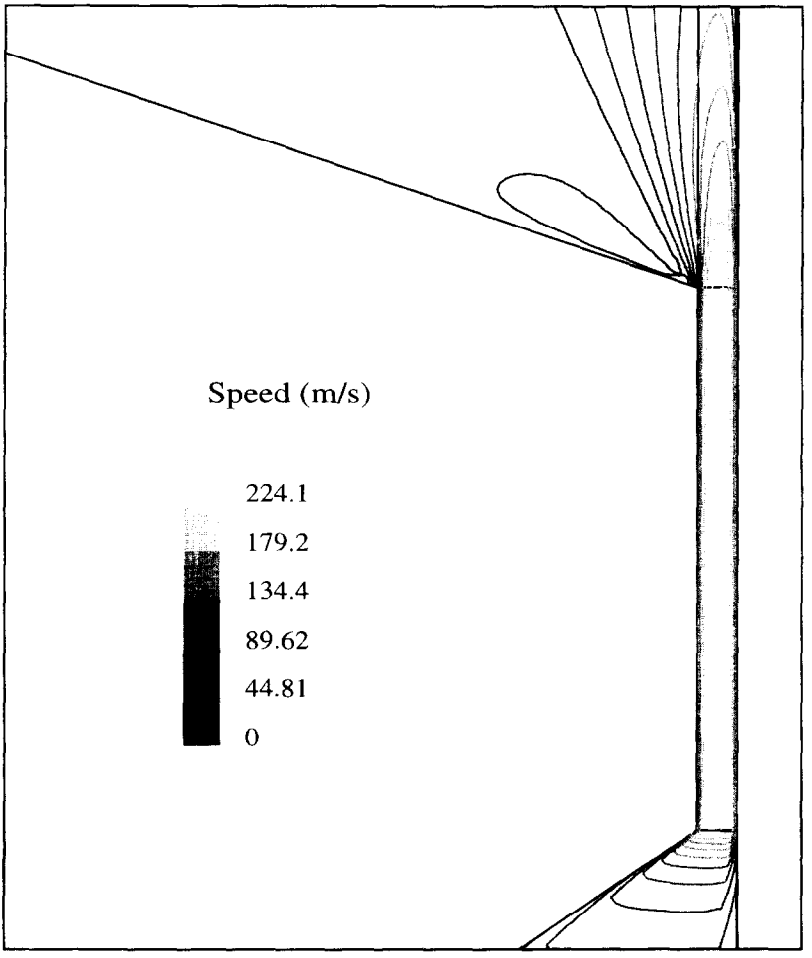

Fig. 5. Velocity contours, 10 μm valve gap.

$$Momentum \quad \frac{\partial(\rho U)}{\partial t} + \nabla\cdot(\rho U \otimes U) - \nabla\cdot(\mu_{\text{eff}}\nabla U) = -\nabla p' + \nabla\cdot(\mu_{\text{eff}}(\nabla U)^{\text{T}}) \tag{7}$$

The modified pressure p' is related to the true pressure by

$$p' = p + \tfrac{2}{3}\rho k + \left(\tfrac{2}{3}\mu_{\text{eff}} - \zeta\right)\nabla\cdot U \tag{8}$$

The k–ε model for turbulent flow assumes

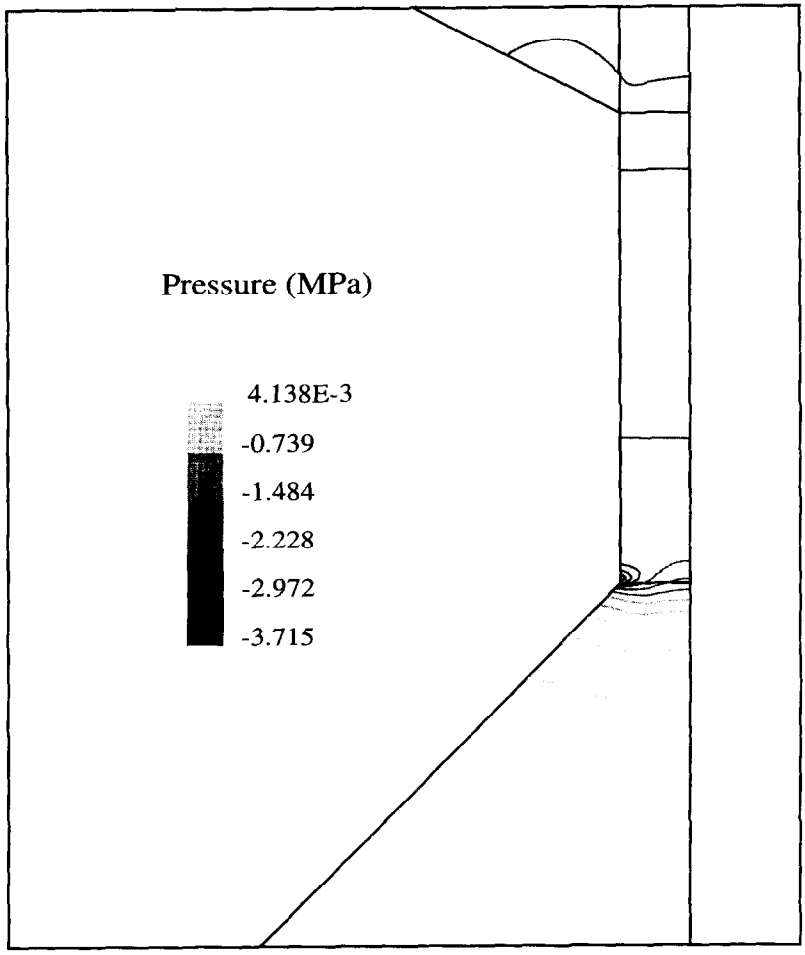

Fig. 6. Pressure contours in valve gap, 30 μm valve gap.

$$\mu_{\text{eff}} = \mu + \mu_{\text{T}} \text{ where } \mu_{\text{T}} = C_{\mu}\rho\frac{k^2}{\varepsilon} \tag{9}$$

Equations for turbulent kinetic energy and turbulent energy dissipation are

$$\frac{\partial(\rho k)}{\partial t} + \nabla\cdot(\rho U k) - \nabla\cdot\left(\left(\mu + \frac{\mu_{\text{T}}}{\sigma_{\text{k}}}\right)\nabla k\right) = P - \rho\varepsilon \tag{10}$$

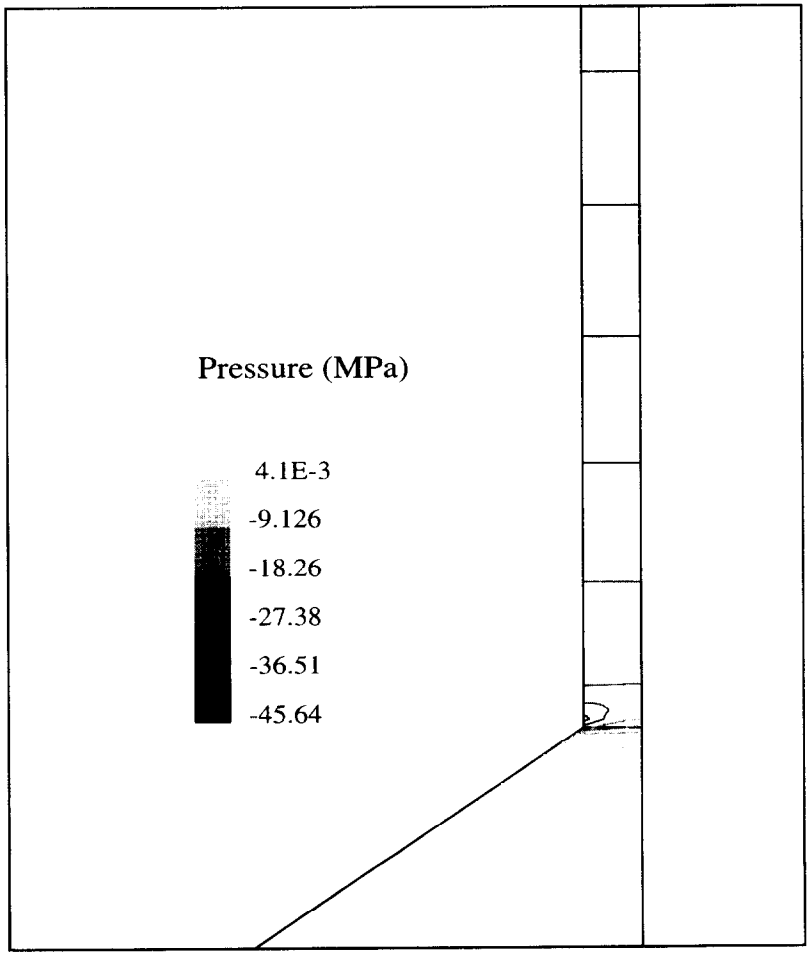

Fig. 7. Pressure contours in valve gap, 10 μm valve gap.

$$\frac{\partial(\rho\varepsilon)}{\partial t}+\nabla\cdot(\rho U\varepsilon)-\nabla\cdot\left(\left(\mu+\frac{\mu_T}{\sigma_\varepsilon}\right)\nabla\varepsilon\right)=C_1\frac{\varepsilon}{k}P-C_2\rho\frac{\varepsilon^2}{k} \tag{11}$$

where P is the shear production defined by

$$P=\mu_{\text{eff}}\nabla U\cdot(\nabla U+(\nabla U)^T)-\tfrac{2}{3}\nabla\cdot U(\mu_{\text{eff}}\nabla\cdot U+\rho k) \tag{12}$$

The Simplec pressure correction algorithm was used.A two-dimensional model of the valve was undertaken on a multi-block grid. This was primarily to save on

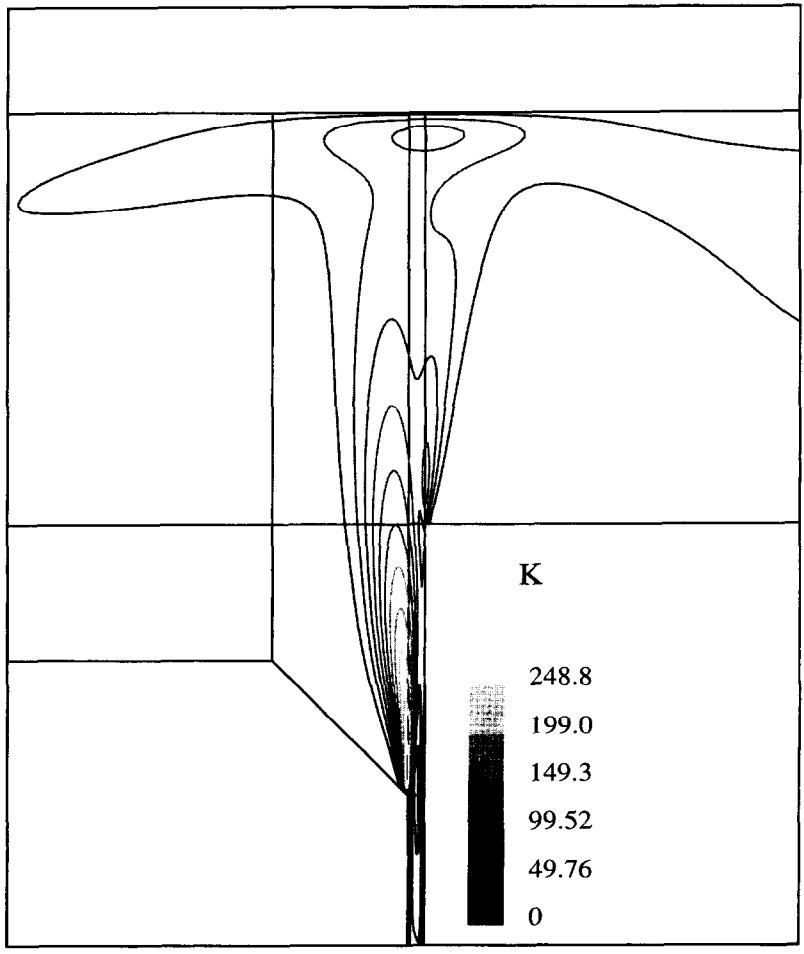

Fig. 8. Turbulent kinetic energy contours, 30 μm valve gap.

calculation times and reduce the computer memory needed. Because of the very small valve gaps that were investigated the grid had some very large differences in scale. For example, the valve gap was around 10–30 μm and the domain length was 18 mm, this required a large number of cells to produce a suitable grid. Large gradients in the valve gap region required a fine grid further complicating the modeling. The final model had 10 cells in the valve gap, the limiting factor became computer memory. The difference between the pressure drop calculated for 5 cells and 10 cells in the valve gap was no more than 3%.

Four types of boundary conditions were applied. The pipe inlet was a uniform velocity profile of 2.841 m/s (Kleinig *et al.*, 1995), giving a flow rate of 4.93×10^{-3} m^3/s for all valve gaps. The value of k at the inlet was set from $k_{in} = 0.002U_{in}^2$ and epsilon was found from $\varepsilon_{in} = k_{in}^{1.5}/0.3D$. The near wall regions

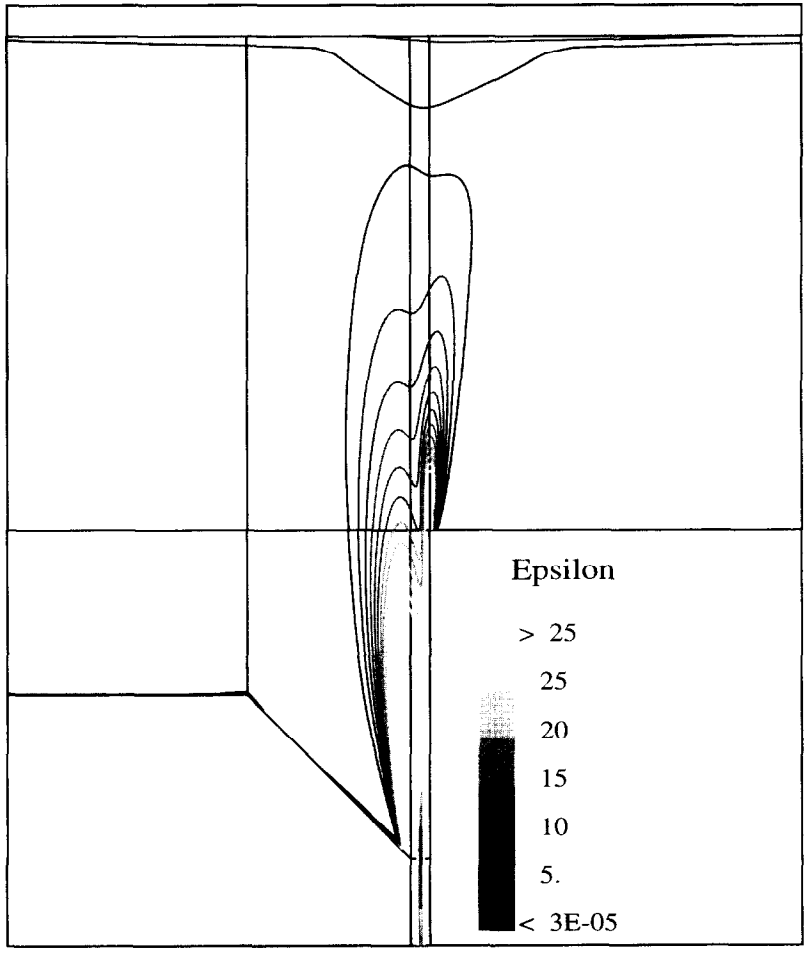

Fig. 9. Turbulent energy dissipation contours, 30 μm valve gap.

were set to the standard wall law profile. The pipe center was a symmetry boundary condition with special treatment of the coincident grid points at the valve centre line. At the outlet, the flow was assumed to be fully developed, thus there was flow only parallel to the pipe axis.

Under-relaxation was applied to each of the equations. Linear relaxation was used i.e. $\phi_{new} = \psi \cdot \phi^*_{new} + (1-\psi) \cdot \phi_{old}$, where ϕ^*_{new} is the calculated value and ϕ_{new} is the value used in the next iteration. The program defaults were found to be suitable for most runs, however at the smaller valve gaps, adjustment of the relaxation parameters was required. Generally, ψ varied between 0.3 and 0.7 for the momentum equations. For pressure, it was found that no relaxation or very light relaxation was the best ($0.9 \leq \psi \leq 1.0$). The turbulence equation relaxation could be quite 'tricky', especially at the start of computation. Large relaxation factors were applied at the

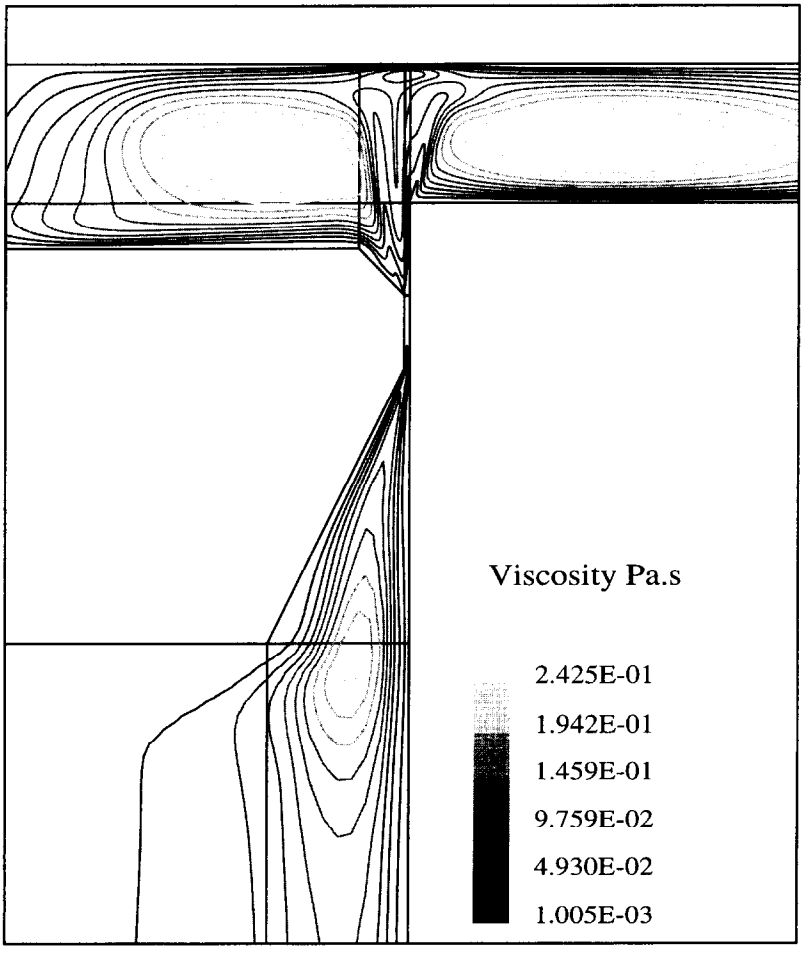

Fig. 10. Effective viscosity contours, 30 μm valve gap.

start of a run, i.e. ψ was between 0.1 and 0.3. It was increased to 0.5 to 0.8 near the end of calculations.

The criteria for convergence was tested by normalizing the errors in each one of the equations ρ, u, v, k and ε. For the continuity equation (ρ, mass), this involved normalizing the error in mass (sum of the absolute mass error in each cell), with the mass flowing into the valve. The mass error in the domain was reduced to 1% for the larger valve gaps (20–30 μm) and 3–5% for the smaller valve gaps, i.e. a very small generation or loss of mass. For the other equations the errors were normalized with the flow of the variable into the valve and also at a region more typical of the variable in the entire domain. For ε this region was the flow of turbulent energy dissipation across the valve gap. This was required because in value of ε flowing into the valve was hundreds of times lower than that in the valve gap.

The domain was broken into 12 blocks to accommodate the changes in orientation and scale. This allowed for 10 cells in the valve gap without the grid becoming too non-uniform. An overview is presented in Fig. 2. Overall, the number of cells averaged around 20,000. When each problem was set up they were run on an RS\6000 computer for between 1,500–3,000 iterations. This required approximately 44 Mb of memory and 12–36 h per run.

RESULTS AND DISCUSSION

The results of the computations have been compared with those of Kleinig *et al.* (1995), and Kleinig and Middelberg (1996). Their results were for peak pressure over each run cycle. Remarkable agreement was found in the pressure drops predicted and those found by the experiments. Figure 3 shows the relationship between pressure drop and valve gap. The calculated results show the same trend as the experiments as well as being of quantitatively similar numerical values. This indicates that the model can at least predict the pressure drop across the valve, without involving assumptions used in previous mathematical analysis.

Figures 4 and 5 show the velocity contours in the valve gap for 30 μm and 10 μm gaps. The horizontal scale is expanded in Fig. 5 so that the contours in the gap can be seen better. The contour shades indicate more than one value, e.g. in Fig. 4 the darkest shade represents 0–14.48 m/s. Both figures show rapid acceleration in the valve gap and a quick development of velocity profiles. In the gap region there are large velocity gradients in the region of the wall. This can affect models of break-up based on shear. Fig. 5 also shows the velocity near the impact ring. The flow splits in two, one portion flows out of the valve. The rest forms a circulation zone between the impact ring and valve seat.

It has been noted that the vigorous smashing action of the fluid upon the impact ring may form another major force for particle breakage. Re-agglomeration may also be occurring as the particles in the 'circulation zone' are thrown back into the stream of particles from the valve gap. These effects seem to be absent in previous work.

Figures 6 and 7 display the pressure contours in the valve gap for gaps of 30 and 10 μm. The values are relative based on the inlet pressure which was set as 0. All pressures could be scaled to realistic values by taking the calculated outlet pressure and adding a constant up to the actual outlet pressure. The horizontal scale is expanded in both plots ($\times 2$). The pressure drop in the inlet of the valves is easily

seen. This pressure drop causes the increase in the velocity of the fluid. The pressure drop due to friction is most significant in Fig. 7 (10 μm) with a fairly constant pressure decrease with distance through the valve. This information is important as there are a number of relationships developed for cell disruption based on pressure. A low pressure region is seen at the inlet of the valve gap; this was also seen in a simplified laminar flow model by Kleinig *et al.* (1995). A slight recovery in pressure is obtained at the outlet of the valve because of the slowing of the flow (not shown).

One of the major opportunities the modeling reveals is the use of turbulence energy and its dissipation rate as variables for modeling disruption. Contours of turbulent kinetic energy (k) are shown in Fig. 8 and those for turbulence dissipation rate (ε) in Fig. 9 for the 30 μm gap. k is very low in the valve gap as is expected due to the viscous dominance, correspondingly ε is very high. At the end of the valve gap the fluid jets into relatively still fluid causing both high values of k and ε. The same effect occurs at the end of the valve head. The values of k and ε can hopefully be used to further the work by Zhang and Thomas (1995), who developed cell-turbulence interaction concepts.

One aspect which is of concern to all CFD is the turbulence model. This is especially true in the conditions of this investigation. The flow domain contains regions of turbulent, transitional and laminar flow (valve gap). The inlet pipe has a Reynolds number of 13,306 which is just turbulent. The valve gap however is so small that the turbulence is 'damped' out, even though the velocity increases so markedly. This is evident in Fig. 10 as the effective viscosity reduces to the laminar viscosity in the valve gap. Coming out of the valve gap the flow expands causing regions of high turbulence due to the flow being free of the wall effects that dominate in the valve gap. This suggests that an area for improvement is a turbulence model more capable for low Reynolds flows. As far as the pressure drop is concerned the k–ε model used here appears to be sufficient.

CONCLUSIONS

The results of the modeling show that the valve can be modeled by the CFD code. The resulting information compared well to that of previous experimental and theoretical investigators. Pressure drop has been correctly predicted. The modeling gives the first detailed information available on speeds and turbulence in disruption valves. The possibilities exist to use the information to produce models for cell and fat globule disruption based on basic flow variables. This can further lead to the complete modeling and design of valves before testing is done on prototypes, avoiding considerable time and costs.

ACKNOWLEDGEMENTS

This modeling would not have been possible without funding from the Engineering Dean's Scholarship, as well as funding from the Chemical and Materials Department. We would like to thank Prof. G. D. Mallison for his help with the basics of CFD.

REFERENCES

Kawaguchi, T. (1971). Entrance loss for turbulent flow without swirl between parallel discs. *Bull. JSME*, **14**, 355–363.

Kleinig, A. R., Ide, B. H. & Middelberg, A. P. J. (1995). High-pressure homogenizer valve mechanics. In *CHEMECA '95, 23rd Aust. Chem. Eng. Conf.*, Vol. 3, pp. 50–55.

Kleinig, A. R. & Middelberg, A. P. J. (1996). Fluid mechanics of a high-pressure homogenizer. In *The 1996 IChemE Res. Event, 2nd Euro. Conf. for Young Res. in Chem. Eng.*, Vol. 1, pp. 109–111.

Launder, B. E. & Spalding, D. B. (1974). The numerical computation of turbulent flows. *Computer Methods in Applied Mechanics and Engineering*, **3**, 269–289.

Nakayama, Y. (1964). Action of the fluid in the air-micrometer (3rd report, characteristics of double-disc nozzle no. 1, in the case of compressibility being ignored). *Bull. JSME*, **7**, 698–707.

Phipps, L. W. (1974). Cavitation and separated flow in a simple homogenizing valve and their influence on the break-up of fat globules in milk. *Journal of Dairy Research*, **41**, 1–8.

Phipps, L. W. (1974). Some operating characteristics of a simple homogenizing poppet valve; pressure profiles and separation: Zone of fat globule dispersion. *Journal of Dairy Research*, **41**, 339–347.

Phipps, L. W. (1975). The fragmentation of oil drops in emulsions by a high-pressure homogenizer. *Journal of Physics D: Applied Physics*, **8**, 448–462.

Zhang, Z. & Thomas, C. R. (1995). Direct cell-eddy interactions in turbulent flows. In *CHEMECA '95 23rd Aust. Chem. Eng. Conf.*, Vol. 3, pp. 98–103.